The effect of heat treatment and cooling rate on the properties of Lightweight aggregates

Markus Bernhardt[a], Hilde Tellesbø[b], Harald Justnes[c], Kjell Wiik[a]

[a] Department of Materials Science and Engineering, Norwegian University of Science and Technology, NO-7491 Trondheim, Norway.

[b] Weber Leca Rælingen, NO-2008, Fjerdingby, Norway

[c] SINTEF, Building and Infrastructure, NO-7491, Trondheim, Norway

Department of Materials Science and Engineering, Norwegian University of Science and Technology, NO-7491 Trondheim, Norway.

Corresponding author: Kjell Wiik, Department of Materials Science and Engineering, Norwegian University of Science and Technology; Sem Sælands vei 12, 7491 Trondheim, Norway. Email: kjell.wiik@ntnu.no, phone: +4773594082

Abstract

Lightweight aggregates (LWA) were produced from clay in the laboratory. After firing different heat treatments and cooling rates were applied and the resulting material was investigated with respect to strength and microstructure. Fast cooling led to the formation of micro cracks and weakened the material whereas slow cooling enhanced the strength of LWA. The residence time at temperatures between 700°C and 900°C led to differences in average oxidation state of iron in the matrix phase leading to substantial changes in thermal behaviour of the matrix phase. The combination of a highly oxidized shell and a reduced core

proved to enhance the strength of LWA. A two hour heat treatment at 800°C in air combined with a subsequent slow cooling rate (0.7°C/min) applied to LWA produced in an industrial rotary kiln led to a strength increase of 114 % compared to material of the normal production without changing any other property.

Keywords: Lightweight aggregate, heat treatment, cooling rate, toughening, glass phase

1 Introduction

Artificial lightweight aggregates (LWA) are produced from natural raw materials like clay or slate or industrial waste products like fly ash or sludge [1-4]. The industrial production of LWA takes place in rotary kilns where the raw material is fired at temperatures up to1300ºC. Expansion occurs due to the evolution of gases at a temperature where the material is in a visco-plastic, partly molten state and able to trap gases [5]. After cooling the molten matrix basically remains as a glassy phase which usually incorporates a variety of different crystalline compounds depending on the composition of the raw material as well as the temperature history [5, 6].

A certain mechanical stability is required for LWA in most of their applications. E.g. foundations for houses or roads or as aggregate in lightweight aggregate concrete (LWAC) [7-10]. Enhancing the mechanical properties of LWA will improve the current applications of LWA such as e.g. LWAC [11-13] and potentially also open up for new and novel applications.

The aim of the present study was to improve the mechanical properties of lightweight aggregates made from clay with a special focus on the glass phase. The glass phase forms a

continuous three dimensional network after firing and consequently plays a major role with respect to mechanical strength. Generally, the properties of glass are influenced by its thermal history in different ways [14]. Pre-tensioning through fast cooling from the upper limit of the glass transition temperature (T_g) or above is a common technique to toughen flat glass. This method introduces permanent compressive stresses into the surface of the sample, hence protecting the glass from failure. On the other hand glasses are also susceptible to thermal shock (cooling below T_g) leading to micro crack formation in the materials caused by temporary stresses arising from local temperature and volume differences and inherently worsen the mechanical properties [14].

In the first part of this study glass transition temperatures, T_g, and softening temperatures, T_s, of the glass phase (synthesized) as well as the "true" matrix phase of LWA in dependence of the oxidation state of iron were determined by dilatometry. In the second part, heat treatments at different temperatures and residence times combined with variable cooling rates were applied to LWA (produced in the laboratory), basically aiming at investigating the role of T_s and T_g and targeting possible combinations of temperature and residence time corresponding to enhanced mechanical strength. This approach is quite similar to techniques applied in the glass industry. Possible mechanisms responsible for the strength of LWA are put forward and discussed. Finally, the most successful heat treatment and cooling procedure with respect to mechanical strength observed on a laboratory scale was also tested on an industrial scale.

2 Material and methods

2.1 Raw material

The utilized raw material was clay blended with 1 wt.-% waste motor oil as expansion agent. Homogenization of the clay as well as the mixing of oil into the clay was performed by shaft mixers in an industrial production line at Saint-Gobain Weber in Norway. The chemical and mineralogical composition of the clay was determined by an external research company called "IBU-tech advanced materials AG" using gravimetry, wet chemical quantification methods and X-ray diffraction and are given in Tab. 1.

chemistry	SiO_2	Al_2O_3	Fe_2O_3	K_2O	MgO	CaO	Na_2O	TiO_2	$LOI_{(1000°C)}$
	59	18	7	4	3	2	1	1	5
mineralogy	quartz	plagioclase	orthoclase	amphibole	illite/ muscovite	chlorite	Fe-oxihydrate		
	17	19	6	4	40	10	4		

Table 1: Chemical and mineralogical composition of the raw clay, the results are normalized to 100 % and are presented in wt.-%

2.2 LWA manufacturing

Lightweight expanded clay aggregates were produced manually in the laboratory. Clay pellets of consistent size and weight were rolled by hand, dried at 105°C, pre-heated for 2 hours at 250°C and finally fired for 8 minutes at 1120°C in a chamber furnace. Different cooling rates and post-burning heat treatments were applied. Tab. 2 gives an overview of the notation of samples and the thermal treatments after firing and Fig. 1 illustrates the thermal profiles. The first number in the sample name refers to the temperature in °C of the last applied heat treatment and the last number indicates the subsequent cooling rate in °C/min. In case of extraordinary long heat treatments (18 hours) the residence time is given as a first number.

Samples that were kept at higher temperatures for a certain time (900-0.7, 800-0.7, 700-0.7, 18h-800-0.7 and 800-900) were transferred from the burning kiln, where expansion took place, to another chamber furnace (pre-heated at the desired temperature) directly after firing. In order to minimize the temperature drop during transportation between the furnaces the fired pellets were carried on a refractory plate which was kept together with the pellets in the burning kiln. The production (expansion) was done in a batch process of about 10 pellets at a time. In order to ensure a sufficient amount of pellets for each sample series several batches had to be produced. In case of the heat treated samples, several batches of pellets were collected in the second chamber furnace (at constant temperature) before starting the cooling procedure. Consequently, the residence time of the pellets within a series varied between 15- and 120 minutes as stated in Tab. 2. In Fig. 1 just an intermediate residence time of 90 minutes is given for sake of clarity. To obtain very high cooling rates (about 900°C/min, accounting for the 800-900- and 1120-900 sample) the pellets were exposed to a flow of compressed air. The sample 1120-160 was cooled to room temperature after firing without any specific heat treatment and was used as a reference material. Cooling rates of the samples 1120-160, 800-900 and 1120-900 were approximated from the measured time it took to cool the pellets to room temperature.

In addition to the laboratory samples, LWA produced in an industrial rotary kiln were also heat treated and compared to LWA from the normal industrial production. About 2 litres of LWA were taken from the kiln head (end of the rotary kiln) and quickly transferred to a chamber furnace; kept for 2 hours at 800°C and subsequently cooled to room temperature at a rate of 0.7°C/min (same heat treatment as used for the sample 800-0.7). The reference material was taken from a conveyer belt after the cooler (in the normal production line) about 20 min after the material was taken from the kiln head. 20 min is the approximate time it takes

for the material to pass through the cooler and with a burning temperature of approximately 1200°C in the kiln the cooling rate of the reference material was approximated to 60°C /min.

sample	temperature profile	cooling rate [°C/min]	profile number in Fig. 1
1120-160	8 min - 1120°C	160	1
900-0.7	8 min - 1120°C / 15-120 min - 900°C	0.7	2
800-0.7	8 min - 1120°C / 15-120 min - 800°C	0.7	3
700-0.7	8 min - 1120°C / 15-120 min - 700°C	0.7	4
18h-800-0.7	8 min - 1120°C / 18 h - 800°C	0.7	5
1120-900	8 min - 1120°C	900	6
800-900	8 min - 1120°C / 15-120 min - 800°C	900	7

Table 2: Notation, temperature profiles and cooling rates for all samples produced in the laboratory. The sample 1120-160 was used as a reference.

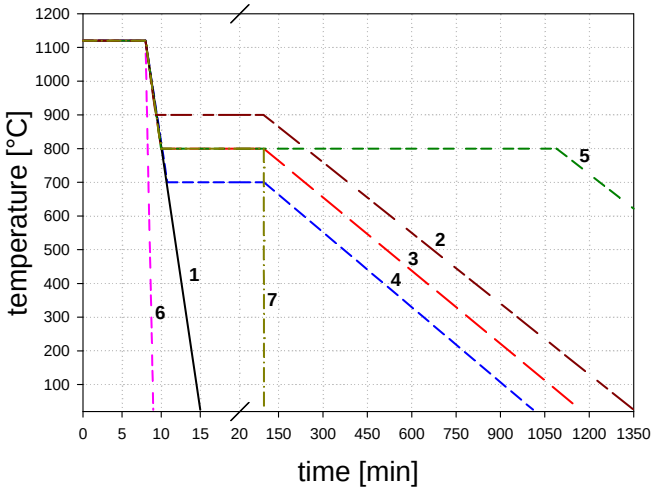

Figure 1: Temperature profiles for all the samples produced in the laboratory. The numbers refer to the samples given in Tab. 2. Profile 1 refers to the sample 1120-160 which was used as a reference. (Note that the abscissa scale is broken at 20 minutes).

2.3 Synthesis of the glass phase

The composition of the glass phase was approximated from XRF (X-ray fluorescence) of the reference LWA taking into account that approximately 10 % of the matrix phase is crystalline quartz. The results were confirmed by EDS (energy dispersive spectroscopy) and the composition of the glass phase is given in Tab. 3. The glass was produced under reducing conditions by the company Saint-Gobain-Weber. The redox state ($Fe^{2+}/(Fe^{2+}+Fe^{3+})$) was determined to be 0.85 by the supplier using wet chemical analysis (titration) and XRF. An oxidized version of the glass phase was produced by milling the reduced glass to a powder, keeping it at 800°C for 18 hours at oxidizing conditions (air) and subsequently sintering at 1150°C for 8 hours and finally cooling at a rate of 200°C/min.

SiO_2	Al_2O_3	Fe_2O_3/FeO	CaO	MgO	K_2O	Na_2O
58	20	9	3	3	5	2

Table 3: Approximate composition of the glassy phase based on EDS and XRF. Results are presented in wt.-%.

2.4 Material testing

The thermal expansion behaviour and softening temperatures (T_s) of the glass phase and LWA matrix phase were determined with a DIL 402C pushrod dilatometer from Netzsch and an optical dilatometer (type misura HSM CDHT 1600-3002) from Expert system solutions. A pushrod dilatometer exerts a small force on the test piece whereas the optical dilatometer does not affect the sample mechanically but shows a lower accuracy. The utilized test pieces of the glass were blocks of 0.5-1 cm shaped by grinding with SiC paper. Test pieces of the LWA matrix where cut from the centre of an expanded LWA and gently shaped by grinding with

SiC paper. The results were highly porous blocks of approximately 1 cm length shown in Fig. 2. The reduced sample was taken from the core of the 800-0.7 sample and the oxidized sample from the core of the 18h-800-0.7 sample. Heating rates were 5 K/min in the pushrod dilatometer and the atmosphere was argon (quality 5.0) for the reduced samples and synthetic air (quality 5.0) for the oxidized samples. The heating rate used in the optical dilatometer was chosen lower (1.5 K/min) to reduce the inherent background noise of the instrument and the atmosphere was ambient air for all samples since the instrument did not provide a gas tight sample chamber.

LWA produced in the rotary kiln consisted of pellets of up to 20 mm diameter. The investigated fraction of both the reference and the heat treated LWA was 10-12 mm (sieved).

The average dry particle density, $\rho_{particle}$, of LWA was determined by sand pycnometry. At least 20 individual pellets were put into a flask and covered with a defined amount of fine sand to measure the volume. The particle density was calculated by dividing the mass of the material by the measured volume.

Helium pycnometry was used to determine the density of the matrix phase, ρ_{matrix}. Each density measurement was performed by milling a couple of pellets to a particle size < 36 micron and subsequently assessing the density in an AccuPyc 1330 helium pycnometer from micrometics.

The average porosity, P, in per cent of each sample is calculated by Eq. 1.

$$P = 100 \cdot \left(1 - \frac{\rho_{particle}}{\rho_{matrix}} \right) \tag{1}$$

Single pellet strength was determined by uniaxial compression between 2 parallel rigid platens. The diameter of every single pellet was measured with a calliper before the granule

was placed on the bottom plate of a press. Compression was performed with a constant speed of displacement of 2 mm per minute until a crack ruptured the pellet into at least two pieces. The applied load at failure, F_{crit}, of at least 20 pellets was recorded for each set of experimental parameters (sample series). The test equipment for samples produced in the laboratory was a TIRATest 2420 press including a load cell with a maximum capacity of 1 kN. The platen material was stainless steel. The samples produced in the rotary kiln were tested with a press made by "Instron ®" coupled to a load cell with a maximum capacity of 1 kN. The platen material was alumina. It is assumed that the difference in platen material did not affect the strength testing results.

The solid strength, σ_{crit}, of each sample series was calculated from the average load at failure, F_{crit}, the volume fraction of solid material within the pellet, $\rho_{particle} / \rho_{matrix}$, and the average diameter, D, using Eq. 2.

$$\sigma_{crit} = \frac{F_{crit}}{D^2 \cdot \left(\rho_{particle} / \rho_{matrix}\right)^{2/3}} \tag{2}$$

The result of Eq. 2 is a strength value which is independent of the total porosity, P [15], and consequently allows a comparison of the strength of the matrix phase.

Solid strength results are presented in dependency of the "solid diameter", d, which is the theoretical diameter of a pellet without any porosity and is calculated by Eq. 3.

$$d = D \cdot \left(\frac{\rho_{particle}}{\rho_{matrix}} \right)^{1/3} \tag{3}$$

Prior to catastrophic failure, all pellets will suffer a certain "crumbling" (apparent plastic deformation) at the contact point between platens and pellet. The radius, a_c, of this

"crumbled area" at the point of failure is important for the comparison of strength values of different samples. a_c can be approximated from the average anvil displacement at failure, x, and the initial average radius, R, of a sample by Eq. 4, assuming a perfect sphere and equal damage/crumbling at the top and at the bottom [15].

$$a_c = \left(R^2 - (R - \frac{x}{2})^2 \right)^{\frac{1}{2}} \quad (4)$$

The mineralogical composition of selected samples was determined by powder X-ray diffraction (XRD) using a D8 focus (Siemens) with Cu Kα radiation and operating parameters of 40 mA / 40 kV, step size 0.02° 2 theta and 1 second step time. In order to investigate differences between the matrix phase in the core and shell of LWA the denser shell was carefully removed from the core using a knife. The pieces of several pellets were then milled and homogenised with a hand mortar prior to XRD-analysis.

The microstructure of selected samples was investigated using a scanning electron microscope (SEM) from Hitatchi (C-3400N). For this type of investigation single pellets were cut in half, embedded in epoxy resin, polished and sputtered with carbon.

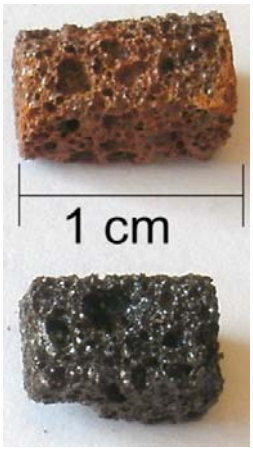

Figure 2: LWA test pieces for the dilatometer investigations. The upper test piece (red) was cut from the core of the 18h-800-0.7 sample and the lower test piece (black) was cut from the core of the 800-0.7 sample.

3 Results and discussion

3.1 Dilatometer analysis of the synthesized glass and the LWA-matrix phase

The purpose of the dilatometer analysis was to obtain approximate values for the dilatometric softening temperature, T_s, and the glass transition temperature, T_g, of the glass phase of LWA. T_s is defined as the temperature of maximum expansion in a pushrod dilatometer [14]. The T_g will be considered as the temperature where the solid glass begins to behave like a viscoelastic solid during heating and is determined from the dilatometer analysis at the temperature were the elongations of the straight lines of linear thermal expansion (above and below T_g) intercept. As previously stated, the atmosphere inside a LWA pellet is highly reducing whereas the outer part or of the pellet is more oxidizing [3]. Accordingly, iron in the glass phase will increase its oxidation state when moving from the centre (core) to the surface

(shell) of the LWA. The thermal expansion behaviour of the synthesized glass phase in an oxidized and reduced state (determined with a pushrod dilatometer) is given in Fig. 3. The T_g and T_s of the reduced glass were found to be 640°C and 715°C, respectively, whereas T_g and T_s for the oxidized state were found to be 780°C and 870°C. The difference between the thermal expansion below and above the glass transition is less pronounced for the oxidized sample compared to the reduced one (cf. Fig. 3). Furthermore, at temperatures above T_s (870°C) the dimension of the oxidized sample does not decrease as rapidly as the reduced sample but shows merely a plateau before gently decreasing above 960°C. The differences in thermal expansion behaviour at $T>T_g$ is most likely caused by an increased viscosity of the oxidized glass compared to the reduced glass. Crystallization processes or a phase separation of different immiscible glass compositions within the oxidized sample could also cause this type of behaviour. However, no further attention was paid to that phenomenon. Nevertheless, it is obvious that a significant increase in T_g and T_s occurs with increasing oxidation state of iron within the glass phase, consistent with studies on the role of iron in the glass phase reported elsewhere [16, 17].

In order to assess the thermal expansion behaviour, as well as T_g and T_s, of the actual matrix phase of LWA used in the present study blocks of porous matrix material (cf. Fig. 2) were tested under the same conditions as the synthesized glass. The results are presented in Fig. 4 and show that the reduced matrix phase is plastically deformable ($T>T_s$) at temperatures above 700°C and the oxidized matrix phase above 950°C. Unequivocally T_g-temperatures were not obtained, possibly blurred by the heterogeneity of the matrix phase (crystalline phases, micro cracks and some gradients in the oxidation state of iron). The change in slope observed between 550°C and 600°C in Fig. 4 is due to the first order phase transition between low- and high quartz at 573°C [18].

In addition to the pushrod dilatometer experiments the thermal expansion behaviour of the matrix phase was also assessed by an optical dilatometer which does not exert any external force on the sample and the results are given in Fig. 5. The instrument was not gas tight and the measurements were therefore run in air for both the oxidized and the reduced sample. The oxidized matrix phase shows no deformation up to 950°supporting the assumption that the observed shrinkage in the pushrod dilatometer experiment (Fig. 4) is initiated by the force exerted by the pushrod. On the other hand the viscosity is not sufficiently low to enable any expansion from gasses trapped in the pores. The reduced matrix phase starts expanding at 700°C in accordance with the results from the pushrod dilatometer (Fig. 4). At 700°C the reduced glass phase exhibits sufficiently low viscosity and consequently the sample expands as gas trapped inside closed pores expands during heating.

At temperatures above T_s the matrix phase is plastically deformable and at temperatures below T_g stresses can be stored within the matrix [14]. Based on the dilatometer analysis (Figs. 3-5) T_s and T_g of the matrix phase are appointed to 950°C and 780°C for the oxidized state and to 700°C and 640°C for the reduced state.

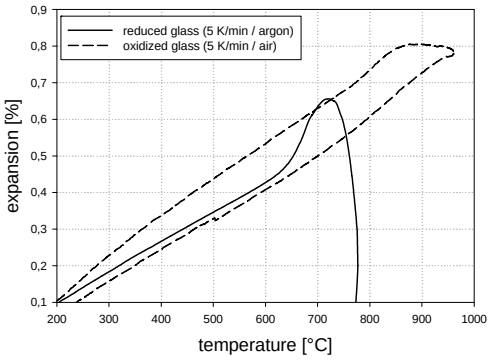

Figure 3: Thermal expansion behaviour of the oxidized- and reduced synthesized glass phase determined in a pushrod dilatometer.

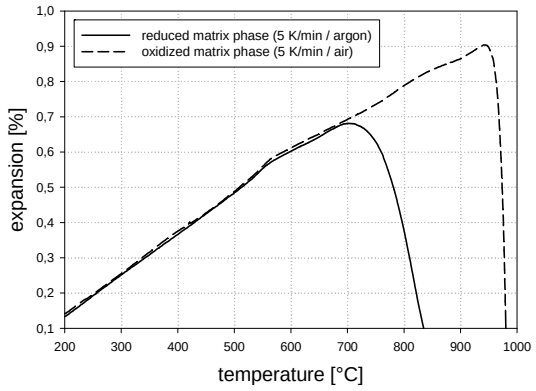

Figure 4: Thermal expansion behaviour of the reduced and oxidized matrix phase of a clay based LWA in a pushrod dilatometer. The applied test pieces are shown in Fig. 2.

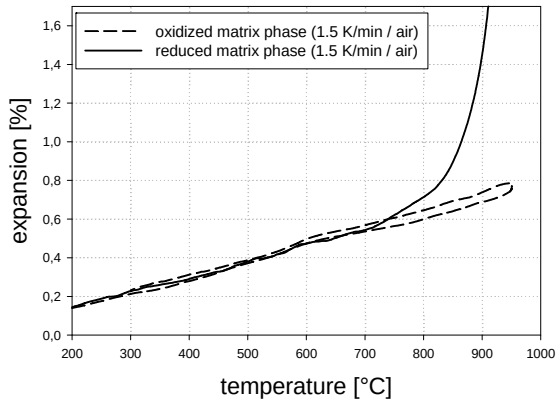

Figure 5: Thermal expansion behaviour of the reduced and oxidized matrix phase of LWA assessed by an optical dilatometer.

3.2 Heat treated LWA produced in the laboratory

3.2.1 The different heat treatments

Different attempts were done to strengthen LWA produced in the laboratory with heat treatments and different cooling rates. The sample 1200-160 was used as a reference since no special heat treatment or cooling was applied.

In order to assess the effect of quenching (fast cooling) on the mechanical properties of LWA the sample 1200-900 was cooled under compressed air directly after firing.

Slow cooling rates (0.7°C /min) were applied after a residence of 15-120 min at 700°C, 800°C and 900°C (and after a long residence of 18 h at 800°C). The temperatures for the heat treatments were set between T_g of the reduced matrix phase (640°C) and T_s of the oxidized matrix phase (950°C). Fig. 6 shows the temperatures of heat treatments in relation to T_s and T_g for both the oxidized- and the reduced matrix phase. With increasing temperature (and residence time) of the heat treatment a higher degree of oxidation of iron within the pellet is expected and consequently a shift in T_g and T_s (as pointed out in chapter 3.1) which again may influence the mechanical properties.

The effect of a heat treatment for 15-120 min at 800°C with subsequent quenching (fast cooling) was investigated as well (sample 800-900).

All the temperature profiles are summarized in Tab. 2 and Fig. 1.

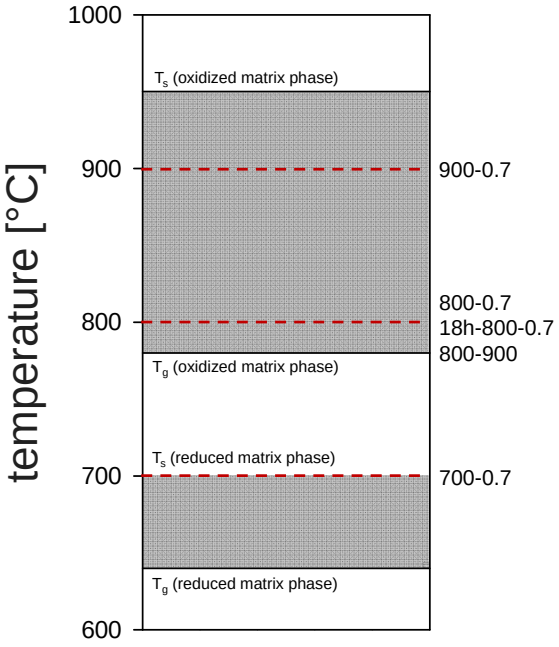

Figure 6: Temperatures of heat treatments in relation to T_s and T_g of both the oxidized- and the reduced matrix phase. The grey areas mark the temperature region between T_s and T_g of the oxidized- and the reduced matrix phase, respectively.

3.2.2 Appearance ("coloration") and oxidation state

The appearance of the core and the outer shell of heat treated samples are given in Fig. 7. The fast cooled samples, 1120-900 and 800-900, are not presented but were similar in appearance to the samples with the same heat treatment but slower cooling rate (1120-160 and 800-0.7). It is evident from Fig. 7 that the outer shell of the LWA shows an increasingly red colouration in the sequence 1120-160, 700-0.7, 800-0.7, 900-0.7, 18h-800-0.7. The core of the samples 1120-160, 700-0.7 and 800-0.7 appear grey-black whereas pellets of the samples 900-0.7 and 18h-800-0.7 show a partly to completely red core. An improved illustration of the colours of the samples 1120-160, 800-0.7 and 18h-800-0.7 is given in Fig. 8. The images are originated

from an optical microscope and the samples are covered with epoxy resin which makes the colours appear more distinct. The colour change from grey-black to red is caused by the oxidation of iron [3] and in the following the colour of the matrix-phase will be used as an indication of its oxidation state. A semi quantitative overview of the oxidation states of all samples is given in Tab. 4. The residence time of 15-120 min at 900°C (referring to the sample 900-0.7) as well as the residence time of 18 hours at 800°C (referring to sample 18h-800-0.7) resulted in almost completely oxidized pellets whereas the remaining samples correspond to a reduced core and a more or less oxidized shell. As previously stated the pellets within the sample series 900-0.7, 800-0.7, 700-0.7 and 800-900 were exposed for 15-120 min to the respective temperature (cf. Tab. 2) and consequently the oxidation state varies within a series. However, the appearance of samples of the same series is quite similar whereas there are distinct differences in appearance between the different sample series (cf. Figs. 7-8).

Figs. 7-8 additionally show that the pore structure and the morphology of the pellets are similar throughout all samples. That implies that the different heat treatments and cooling rates do not change the inner- and outer geometry (pellet diameter, pore-size, pore-distribution etc.) of the pellet.

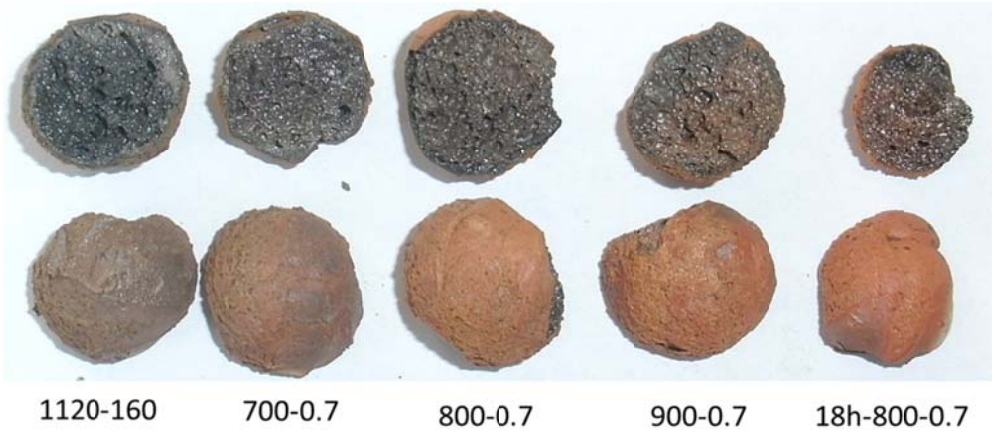

Figure 7: Inner- and outer appearance of LWA pellets after different heat treatments. The diameter of all samples is about 16 mm.

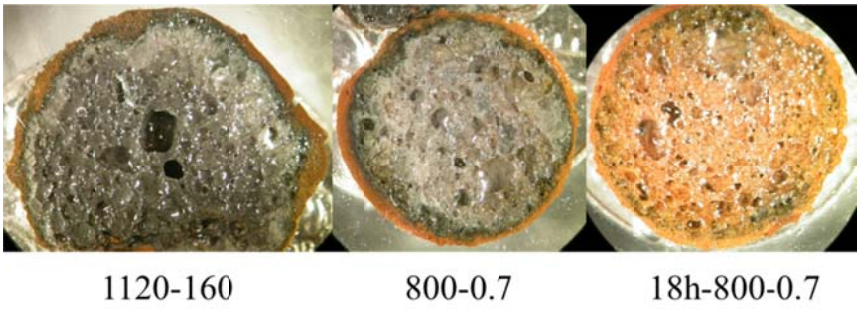

Figure 8: LWA pellets cut in half and covered with epoxy resin under an optical microscope. The diameter of all samples is about 16 mm.

sample	core	shell
1120-160	-	+
900-0.7	++	+++
800-0.7	-	+++
700-0.7	-	++
18h-800-0.7	++	+++
1120-900	-	+
800-900	-	+++

Table 4: Semi quantitative overview of the oxidation state of iron in the matrix phase in core and shell. – reduced (Fe^{2+}), + some oxidation, ++ more oxidation, +++ fully oxidized (Fe^{3+}).

3.2.3 Properties

An overview of the properties of all sample series produced in the laboratory is given in Tab. 5. The diameter, D, porosity, P, solid diameter, d (theoretical diameter without porosity) and the particle density, $\rho_{particle}$, are reasonably constant for all samples. These properties are consequently only influenced by the production parameters that were kept constant for all samples namely the raw material, pelletizing procedure, green pellet size, pre-heating procedure and firing- time and temperature. Smaller variations within the mentioned properties are due to the general high heterogeneity of the material. The assessment of the matrix densities, ρ_{matrix}, did not lead to any significant differences between the different heat treated samples although it is known that cooling rate and oxidation state of glasses can influence their density [14]. The standard deviation of the matrix density of LWA produced from the investigated clay was determined to be about 0.06 g/cm³. Consequently, the given standard deviation may blur small changes which may arise from different heat treatments. To assess this problem, the matrix density of a small amount of reduced matrix material was determined. Subsequently, the same material was oxidized (kept for 18 h at 800°C in air) and the matrix density was determined, again. The results were 2.63 g/cm^3 (± 0.06 g/cm^3) for both samples, thus a change in matrix density through oxidation of the matrix was not detectable on the measuring scale given, hence supporting the assumption that the observed variation in matrix density between the different samples in Tab. 5 was merely due to variations in the raw material.

In order to compare the mechanical properties of the different samples determined by single pellet compression, the ratio between the radius of the contact area between platen and pellet, a_c, and the radius of the pellet, R, has to be considered since it might influence the stress distribution within the pellet. According to Shipway et al. [19, 20] the stresses occurring inside the pellet during compression do not change significantly for $0.2 < a_c/R < 0.6$. Values

of a_c/R are found to be between 0.2 and 0.4 (cf. Tab. 5) for all samples and consequently within the required range.

The solid strength, σ_{crit}, (calculated by Eq. 2) for all samples including porosity values are given in Fig. 9a) and the measured load at failure, F_{crit}, (including the standard deviation) is given in Fig. 9b). F_{crit} and consequently σ_{crit} are influenced by the total amount of solid material under stress during the single pellet compression test (represented by the solid diameter, d) [15]. According to [15] the small changes in solid diameter between the different samples will not influence the results of the strength test significantly. Additionally, all porosity values are fairly similar and consequently the differences in σ_{crit} and F_{crit} between the different samples are not caused by geometrical parameters (D, d or P). However, the standard deviation of F_{crit} is rather large for all samples, due to the brittle nature of the fracture combined with the heterogeneity of the materials. The observed standard deviation (25-40%) correspond to typical values reported for similar materials by Bernhardt et al. [15] and do stress the importance of testing a sufficient (large) amount of samples. Standard deviations of σ_{crit}, d, P and $\rho_{particle}$ are not given since the values result from calculations including the average of several pellets within a sample series and were not measured for every single pellet. However, the standard deviation of σ_{crit} is expected to be in the same order as the standard deviation of F_{crit}. Generally, the standard deviation of all properties is very high which, as previously stated, is due to the heterogeneous nature of the material.

Considering the strength results presented in Fig. 9a) the samples can be divided in two groups: Those that were stronger than the reference sample (1200-160), corresponding to the samples with a slow cooling rate of 0.7 °C/min (900-0.7, 800-0.7, 700-0.7 and 18h-800-0.7) and those that were weaker than the reference, corresponding to the quenched samples with a cooling rate of approximately 900°C/min (1120-900 and 800-900).

The quenched samples show a significantly lower strength than the slowly cooled samples, emphasizing the detrimental effect of micro cracks with respect to strength. However, within each group of samples with the same cooling rate significant variations in strength are observed as well, emphasizing that the formation of micro-cracks is not the only phenomena governing the strength of LWA. This will be further elucidated in the remaining part of the discussion.

sample	diameter D/[mm]	solid diameter d/[mm]	porosity P/[%]	particle density $\rho_{particle}$ / [g/cm^3]	matrix density ρ_{matrix} / [g/cm^3]	load at failure, F_{crit} [N]	solid strength σ_{crit} [MPa]	tested samples	a_c/R
1120-160	16.0 (±0.6)	8.8	83	0.46	2.73(±0.06)	116 (±29)	1.48	70	0.24
900-0.7	16.0 (±0.5)	9.0	82	0.46	2.61(±0.06)	142 (±62)	1.76	20	0.35
800-0.7	15.9 (±0.9)	8.8	83	0.46	2.65(±0.06)	187 (±54)	2.39	40	0.35
700-0.7	16.1 (±0.5)	9.1	82	0.48	2.60(±0.06)	162 (±61)	1.94	20	0.34
18h-800-0.7	16.2 (±0.6)	9.0	83	0.44	2.59(±0.06)	134 (±44)	1.66	20	0.28
1120-900	16.3 (±0.5)	9.0	83	0.44	2.59(±0.06)	54 (±12)	0.67	20	0.20
800-900	16.5 (±0.7)	8.9	84	0.41	2.59(±0.06)	86 (±22)	1.09	20	0.25

Table 5: Overview of the properties of LWA with different heat treatments and cooling rates produced in the laboratory.

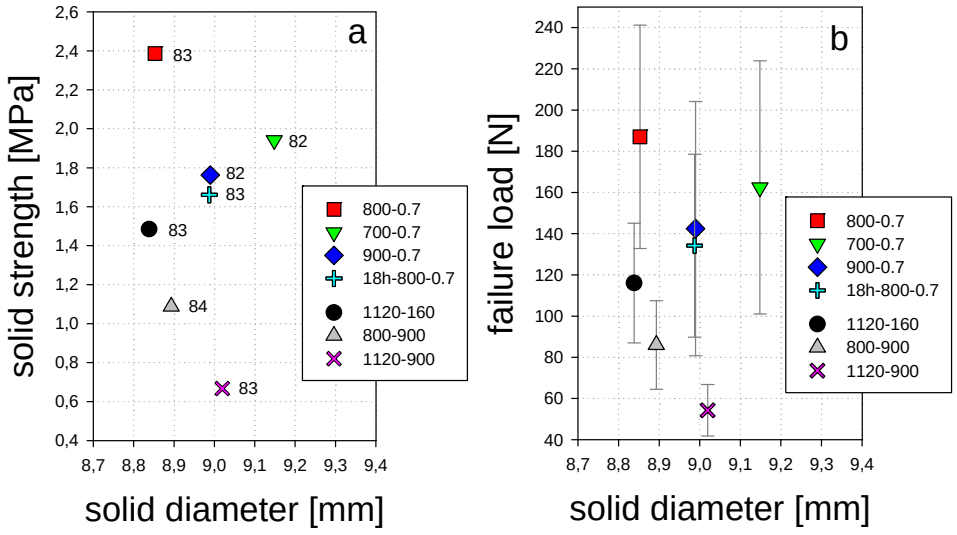

Figure 9: Mechanical properties of samples produced in the laboratory. a): Solid strength including numbers for the porosity in per cent. b): Load at failure in terms of solid diameter, *d*, for the various heat treated samples. Error bars (standard deviation) are included.

3.2.4 Mineralogical composition and microstructure of the samples 1120-160 and 800-0.7

In order to investigate the influence of the mineralogical composition and the micro structure on the strength of LWA the 800-0.7 sample (showing the highest strength) was investigated by XRD and SEM and compared to the reference sample 1120-160.

XRD-analysis of the matrix phase of both the core and the shell of both 1120-160 and 800-0.7 samples are given in Fig. 10. Observed crystalline phases were quartz, feldspar (mainly anorthite), hercynite and hematite. The 800-0.7 sample incorporated enhanced contents of hematite, quartz and feldspar in the shell compared to the core. The presence of hematite (Fe_2O_3) in the shell of 800-0.7 proves the higher oxidation of state of iron in the shell compared to the core as indicated in Tab. 4. No difference was observed between core and shell for 1120-160 in Fig. 10. However, the images of the microstructure in Fig. 11a)-d) reveal that the content of mineral inclusions in the glass phase (continuous grey phase) appears to be slightly higher in the shell than in the core for both samples.

The mineralogical composition as well as the general appearance of the microstructure (distribution of crystals within the glassy phase) of 1120-160 and 800-0.7 is very similar. SEM investigations on the remaining samples showed similar results and are therefore not presented. The appearance (microstructure) of the matrix phase in both core and shell is basically the same as presented in Fig. 11 for the 1120-160- and 800-0.7 sample, respectively.

Consequently, it is unlikely that the observed differences in strength are due to differences in mineralogical composition or micro structure.

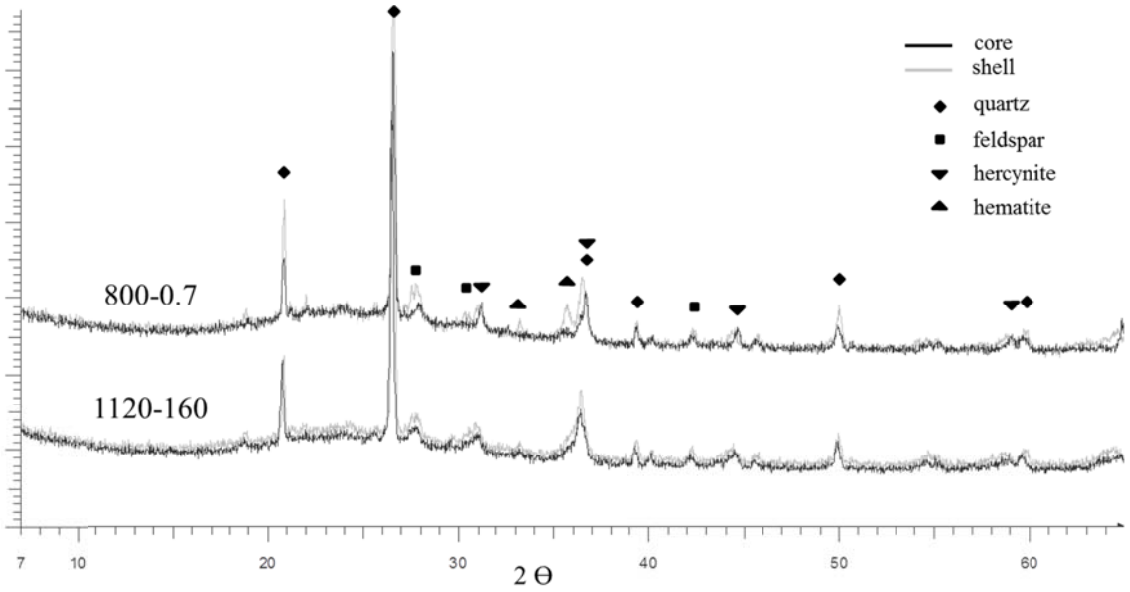

Figure 10: XRD analysis of the core and the shell of the samples 1120-160 and 800-0.7.

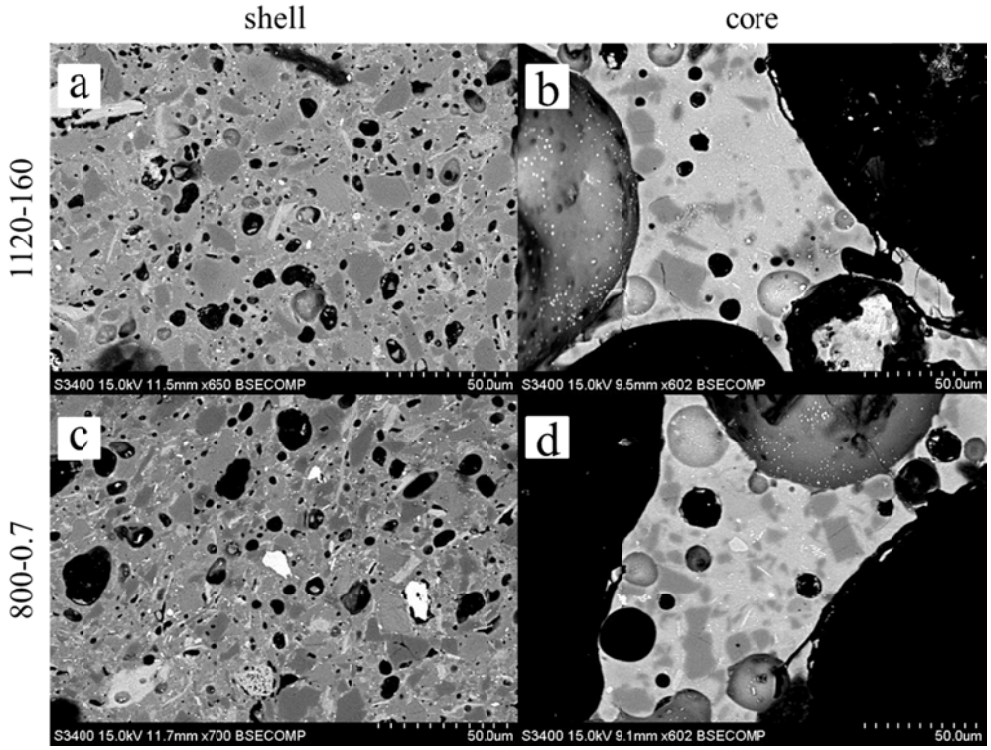

Figure 11: Backscattered electron images of a) the matrix phase in the shell of 1120-160; b) the matrix phase in the core of 1120-160; c) the matrix phase in the shell of 800-0.7 d) the matrix phase in the core of 800-0.7.

3.2.5 Possible toughening mechanisms in heat treated LWA

It has already been discussed that geometrical parameters like sample size, -shape or pore size and pore size distribution do not change significantly throughout the different sample series and consequently will not be responsible for the observed differences in strength. Additionally, no significant differences in mineralogical composition and microstructure were observed by XRD- and SEM-analysis that would explain the observed variations in strength.

It has been pointed out that the formation of micro cracks, due to fast cooling, has a detrimental influence on strength. It is reasonable to assume that the density of micro cracks is quite similar within samples exposed to the same cooling rate. Given that no stresses will be present in the material at temperatures above 780°C (T_g of the oxidized matrix phase) the cooling rate above this temperature does not contribute to the formation of micro cracks. Consequently, the density of micro cracks arising during cooling is quite similar in the 1120-900 and 800-900 –sample (fast cooling) as well as in the samples 900-0.7, 800-0.7 and 18h-800-0.7 (slow cooling). Only the 700-0.7 sample might contain a higher density of micro cracks than the other slowly cooled samples since the slow cooling procedure did not start above T_g of the oxidized matrix phase (780°C, cf. Fig. 6).

Comparing the slowly cooled samples regarding strength it is evident that samples comprising an oxidized shell (high content of Fe^{3+}) and a reduced core (low content of Fe^{3+}), corresponding to the samples 800-0.7 and 700-0.7, show a higher strength than fully oxidized samples (900-0.7, 18h-800-0.7).

Comparing the fast cooled samples regarding strength it is also evident that the sample with a highly oxidized shell and a reduced core (800-900) shows a higher strength than the sample with a less oxidized shell and a reduced core (1120-900).

Hence, it appears that a high content of Fe^{3+} in the matrix of the shell combined with a low content of Fe^{3+} in the matrix of the core lead to enhanced mechanical strength of LWA for a given density of micro cracks. The underlying reason might be the difference in T_s and T_g between the matrix phase incorporating iron in an reduced state and the matrix phase incorporating iron in an oxidized state. The differences in T_s and T_g result in a difference in thermal expansion at temperatures between 950°C and 640°C as shown in Figs. 3-5. Below 640°C both oxidized- and reduced matrix phase are in a solid, rigid state and will show, due to similar chemical composition, quite similar thermal expansion coefficients (TEC). However, at temperatures above T_g the material will behave like a viscose melt and consequently show a higher TEC. Hence, during cooling the core will contract relative to the shell (in case the shell is oxidized and the core is reduced) and induce compressive stresses into the shell that are preserved even after cooling to room temperature. Thus, it seems that oxidation at some intermediate temperature (800°C) just above the T_g temperature for the "oxidized glass phase" (Fig. 6) for some intermediate time (between 15 and 120 minutes) is the most beneficial condition for strengthening the LWA-pellets. Almost complete oxidation (18h-800-0.7 and 900-07) gives less strengthening. It is also seen that less oxidation (700-0.7) also gives less strength than 800-0.7. Finally, we see that enhanced strength is observed even for quenched samples when heat treated at 800°C for optimal time (800-900) compared with non-heat treated sample (1120-900). From these results we propose that there exist an optimum ratio between the thickness of the oxidized shell and the radius of the reduced core which enhance the strength of the pellet when cooled from above the T_g temperature of the "oxidized glass phase". The toughening mechanism is proposed, as stated above, to be due to

compressive forces being induced in the oxidized shell part of the pellet. The final proof, supporting our proposed strengthening mechanism, is yet to be launched, however it is the authors opinion that the present results do form a fruitful starting point for further investigations related to strengthening LWA-pellets.

3.3 Heat treated LWA produced in the rotary kiln

The most successful heat treatment and cooling rate among the laboratory samples was definitely the 800-0.7 sample giving by far the highest strength. Hence, the same conditions were tested also for samples produced in an industrial full scale rotary kiln. The investigated fraction was 10-12 mm (sieved) and the colouration of the pellets after the heat treatment was similar to the samples produced in the laboratory (corresponding to sample 800-0.7; cf. Figs. 7-8). An overview of the properties of reference- (rot-1200-60) and heat treated material (rot-800-0.7) is given in Tab. 6 and the most important properties are given in Fig. 12. No differences between the samples were observed for *D, d, P,* $\rho_{particle}$ and ρ_{matrix} and the ratio a_c/R was within the required range as discussed in *section 3.2.3*. However, the failure load, F_{crit}, and solid strength, σ_{crit}, increased by more than 110 % for rot-800-0.7 compared to rot-1200-60. Moreover, the standard deviation of F_{crit} was reduced from 52 % (of the average value) for rot-1200-60 to 22 % (of the average value) for rot-800-0.7. A reduced standard deviation of F_{crit} corresponds to an increased Weibull modulus, m, describing an enhanced mechanical reliability of brittle materials [21, 22]. The presented heat treatment led to a higher strength increase for samples produced in the rotary kiln (about 110 % strength increase) than for samples produced in the laboratory (about 60 % strength increase). LWA produced in the rotary kiln generally show a quite regular (close to spherical) shell whereas LWA produced in the laboratory comprise a more irregular shaped shell [15]. Since the

stresses will be more evenly distributed throughout the volume of a highly spherical shaped pellet the resulting strength should also be enhanced. The results from the industrial scale experiments do support our assumptions put forward related to the laboratory samples, that there exist an optimal heat treatment (temperature/time) producing LWA with improved mechanical properties. It should be mentioned that the parameters of the optimal heat treatment are likely to be dependent on the diameter of the pellet.

sample	diameter D/[mm]	solid diameter d/[mm]	porosity P/[%]	particle density $\rho_{particle}$ / [g/cm^3]	matrix density ρ_{matrix} / [g/cm^3]	load at failure, F_{crit} [N]	solid strength σ_{crit} [MPa]	tested samples	a_c/R
rot-1200-60	10.8 (±0.5)	5.9	83	0.43	2.62 (±0.06)	101 (±52)	2.86	50	0.32
rot-800-0.7	10.8 (±0.5)	6.0	83	0.44	2.61 (±0.06)	218 (±48)	6.09	50	0.46

Table 6: Overview of the properties of reference- and heat treated LWA produced in an industrial rotary kiln.

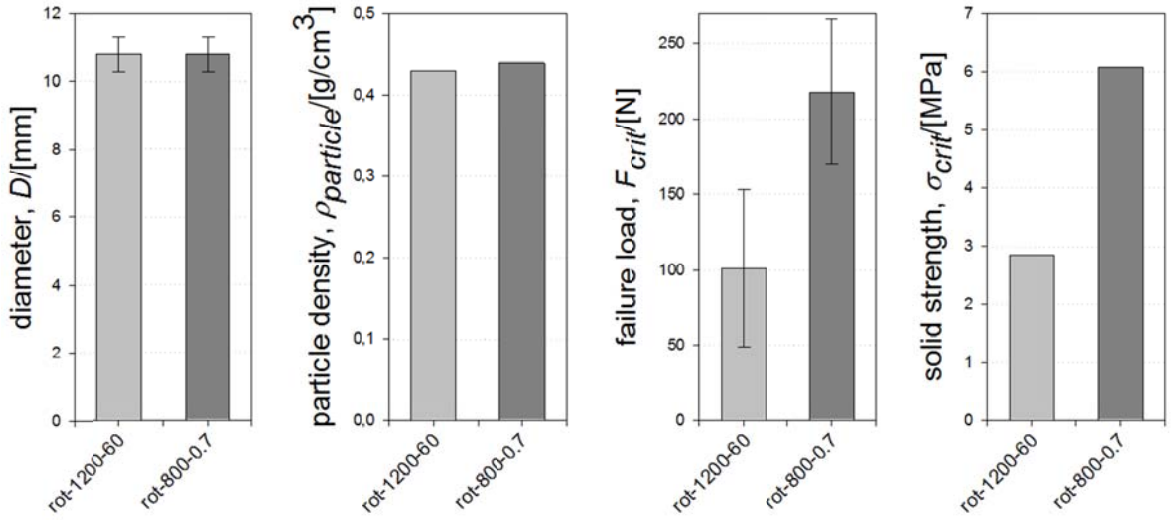

Figure 12: Comparison of the main properties between reference- and heat treated LWA produced in an industrial rotary kiln.

4 Conclusions

Post-burning heat treatments and different cooling rates have been applied to expanded clay aggregates produced in the laboratory in order to enhance mechanical properties. Fast cooling rates weakened the samples due to the formation of micro cracks whereas slow cooling rates increased the strength. Significant differences in thermal behaviour of the matrix phase depending on the oxidation state of iron were observed. A matrix phase constituting mainly Fe^{3+} (indicated by a deep red colouration) softens at approx. 950°C with a corresponding T_g at around 780°C. The matrix phase incorporating mainly Fe^{2+} (indicated by a grey-black colouration) showed a softening point at 700°C and a T_g at 740°C. LWA typically comprise a reduced core and more oxidized shell as a consequence of different atmospheres within and outside the pellet during firing. Through the application of different heat treatments in oxidizing atmosphere the distribution of Fe^{3+}/Fe^{2+} within the pellet is changed resulting in differences in mechanical properties. No significant differences in microstructure, sample geometry or mineralogy were observed due to heat treatments. A reduced core and a highly oxidized shell proved to be the most beneficial constitution with respect to strength.

The best combination of heat treatment (adjusting the oxidation state of core and shell) and cooling procedure (reducing micro cracks through slow cooling) was found to be a residence time of approx. 2 hours at 800°C with a subsequent cooling rate of 0.7/min. Exposing LWA produced in an industrial rotary kiln to the same experimental parameters as for laboratory produced material resulted in a 114 % increase in strength compared to material from the normal production. The observed strength increase did not compromise the resulting density or any other property.

Acknowledgements

Financial support from Saint-Gobain-Weber and COIN (www.coinweb.no) as a part of SINTEF is gratefully acknowledged. Prof. Dr. Hessenkemper and his team of scientists and laboratory personal at the University of Freiberg is acknowledged for their support during this study. Final thanks to Patrick Garnier from Saint-Gobain rechereche for useful discussions and the synthesis of the glass.

Literature

1. Show, KY, Lee, DJ, Tay, JH, Hong, SY, Chien, CY, *Lightweight aggregates from industrial sludge-marine clay mixes.* Journal of Environmental Engineering, 2005. **131**(7): p. 1106-1113.
2. González-Corrochano, B, Alonso-Azcárate, J, Rodas, M, *Production of lightweight aggregates from mining and industrial wastes.* Journal of Environmental Management, 2009. **90**(8): p. 2801-2812.
3. Decleer, J, Viaene, W, *Rupelian Boom clay as raw material for expanded clay manufacturing.* Applied Clay Science, 1993. **8**(2-3): p. 111-128.
4. Arioz, O, Kilinc, K, Karasu, B, Kaya, G, Arslan, G, Tuncan, M,et al.Kivrak, S, *A preliminary research on the properties of lightweight expanded clay aggregate.* Journal of the Australian Ceramic Society, 2008. **44**(1): p. 23-30.
5. Riley, CM, *Relation of chemical properties to the bloating of clays* Journal of the American Ceramic Society, 1951. **34**(4): p. 121-128.
6. de Gennaro, R, Cappelletti, P, Cerri, G, de' Gennaro, M, Dondi, M, Graziano, SFLangella, A, *Campanian Ignimbrite as raw material for lightweight aggregates.* Applied Clay Science, 2007. **37**(1-2): p. 115-126.
7. Hou, Z, Tang, J. *Technical property and applying for bridge deck of ceramsite concrete*. in *ICTE*. 2011.
8. Haug, AK, Fjeld, S, *A floating concrete platform hull made of lightweight aggregate concrete.* Engineering Structures, 1996. **18**(11): p. 831-836.
9. Awwad, MT, *Hot mix asphalt using light weight aggregate concrete.* Journal of Applied Sciences, 2007. **7**(14): p. 1924-1929.
10. Dhir, K, Mays, RGC, Chua, HC, *Lightweight structural concrete with Aglite aggregate: mix design and properties.* International Journal of Cement Composites and Lightweight Concrete, 1984. **6**(4): p. 249-261.
11. Swamy, RN, Lambert, GH, *Mix design and properties of concrete made from PFA coarse aggregates and sand.* International Journal of Cement Composites and Lightweight Concrete, 1983. **5**(4): p. 263-275.
12. Lo, TY, Tang, WC, Cui, HZ, *The effects of aggregate properties on lightweight concrete.* Building and Environment, 2007. **42**(8): p. 3025-3029.
13. Cui, HZ, Lo, TY, Memon, SA, Xu, W, *Effect of lightweight aggregates on the mechanical properties and brittleness of lightweight aggregate concrete.* Construction and Building Materials, 2012. **35**: p. 149-158.
14. Shelby, JE, *Introduction to glass science and technology*2005, Cambridge: Royal Society of Chemistry. 291 s. : ill.
15. Bernhardt, M., Tellesbø, H., Justnes, H., Wiik, K,, *Mechanical properties of lightweight aggregates.* Journal of the European Ceramic Society, 2013, 33, p. 2731-2743.
16. Dingwell, DB, *Redox viscometry of some Fe-bearing silicate melts.* American Mineralogist, 1991. **76**(9-10): p. 1560-1562.
17. Liebske, C, Behrens, H, Holtz, F, Lange, RA, *The influence pf pressure and composition on the viscocity of andesitic melts.* Geochimica et Cosmochimica Acta, 2003. **67**(3): p. 473-485.
18. Okrusch, M, Matthes, S, *Mineralogie*2005: Springer.

19. Shipway, PH, Hutchings, IM, *Attrition of brittle spheres by fracture under compression and impact loading.* Powder Technology, 1993. **76**(1): p. 23-30.
20. Shipway, PH, Hutchings, IM, *Fracture of brittle spheres under compression and impact loading.* Philosophical Magazine A, 1993. **67**(6): p. 1389-1404.
21. Weibull, W, *A Statistical Distribution Function of Wide Applicability.* journal of applied mechanics, 1951. **18**: p. 293-297.
22. Richerson, DW, *Modern Ceramic Engineering* third ed2006: Taylor and Francis group.

Tables

Figure captions

Figure 1

Sdfsdf

Figure 2

Sdfsdf

Figure 3

Sdfsdf

Figure 4

Sdfsdf

Figure 5

Sdfsdf

Figure 6

Sdfsdf

Figure 7

Sdfsdf

Figure 8

Sdfsdf

Figure 9

Sdfsdf

Figure 10

Sdfsdf

Figure 11

Sdfsdf

Figure 12

Sdfsdf

Figure 13

Sdfsdf

Figure 14

Sdfsdf

Figure 15

Sdfsdf

Figure 16

Sdfsdf

Figure 17

Sdfsdf